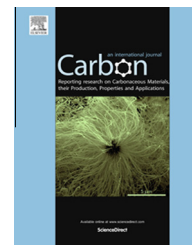


Available at www.sciencedirect.com

ScienceDirect

journal homepage: www.elsevier.com/locate/carbon

Mechanical and electrical properties of aligned carbon nanotube/carbon matrix composites

Zhou Zhou ^a, Xin Wang ^{a,1}, Shaghayegh Faraji ^b, Philip D. Bradford ^b, Qingwen Li ^c, Yuntian Zhu ^{a,*}

^a Department of Materials Science and Engineering, North Carolina State University, Raleigh, NC 27695, United States

^b Department of Textile Engineering, Chemistry and Science, North Carolina State University, Raleigh, NC 27695, United States

^c Suzhou Institute of Nano-Tech and Nano-Bionics, Suzhou 215125, PR China

ARTICLE INFO

Article history:

Received 8 February 2014

Accepted 2 April 2014

Available online 12 April 2014

ABSTRACT

To synthesize carbon nanotube/carbon matrix (CNT/C) composites rivaling or exceeding the mechanical and electrical properties of current carbon fiber/carbon matrix composites, it is essential to align carbon nanotubes in the composite. In this work, we fabricated CNT/polyacrylonitrile (PAN) precursor composites with high degree of CNT alignment, and carbonized and graphitized them at high temperatures. Carbonizing the precursor composites significantly improved their elastic modulus, strength, and electrical conductivity. The matrix was uniformly carbonized and highly graphitized. The excellent mechanical and electrical properties make the CNT/C composites promising for many high temperature aerospace applications.

© 2014 Elsevier Ltd. All rights reserved.

1. Introduction

Carbon fiber reinforced carbon matrix (C/C) composites have attracted tremendous attention from aerospace industries due to their high temperature resistance, high strength, low density, and extremely low coefficient of thermal expansion [1–4]. Compared with carbon fibers, carbon nanotubes (CNTs) possess theoretical strengths that are up to an order of magnitude higher, as well as much higher electrical and thermal conductivities [5–10]. These excellent properties, combined with the high specific surface area, make carbon nanotubes a promising substitute for carbon fibers to meet the challenges of the next generation aerospace technologies.

Inspired by the processing methods of C/C composites, chemical vapor infiltration (CVI) [11–15] and polymer infiltration pyrolysis (PIP) [16–22] methods have been explored to synthesize CNT/C composites. Existence of CNTs was found

to induce graphitization in the matrix under high temperatures [23–27]. Increase in CNT content and degree of alignment were also found to assist the formation of graphitic regions [21,28]. However, the tensile strength and Young's modulus of previously reported CNT/C composites are far lower than those of their C/C counterparts [13]. In addition, the electrical properties were not investigated in detail. Challenges in preparing CNT/C composites with desirable properties include achieving CNT alignment in the structure and homogeneous CNT dispersion in the carbon matrix.

In our previous work [29,30], we developed a one-step winding infiltration method to utilize long and aligned CNT sheets and produced high strength CNT/polymer composites. This method has a unique advantage in producing aligned CNT composite structures, in which nanotubes are uniformly distributed in the matrix. In this current work, we applied this method to fabricate CNT/polyacrylonitrile (PAN) precursor

* Corresponding author: Fax: +1 919 515 3419.

E-mail address: ytzhu@ncsu.edu (Y. Zhu).

¹ Equal contributor to the first author.

<http://dx.doi.org/10.1016/j.carbon.2014.04.008>

0008-6223/© 2014 Elsevier Ltd. All rights reserved.

composites and then pyrolyzed the PAN matrix to make aligned-structured CNT/C composites. PAN is a commercially important polymer, which is used as the predominant precursor for carbon fibers [31]. PAN has the advantages of high carbon yield, simple carbonization process and the ability for surface functionalization [32]. CNTs have been added to PAN fibers in small quantities to improve their properties [33–35]. Other works have studied the stabilization and carbonization of similar materials [28,32,33,36–41], which has been proposed as the next generation carbon fiber products [28,32,38–41]. While that method is very promising for producing carbon fibers, there is a growing interest in making composites that contain no carbon fibers and only a high fiber volume fraction of CNTs as the reinforcing phase. However, there are only limited studies on PAN/C composites films or CNT/C composites produced directly from CNT structures [25,26,36,37]. Producing CNT/C composites by dispersing short CNTs with random orientation and entanglements into carbon precursors and then carbonizing it typically results in very brittle and weak composites.

This work presents a new technique to produce CNT/C composites directly from aligned CNT sheets and PAN precursor, which exhibit mechanical properties superior to other CNT/C composites that are not in a fiber form. The CNT/PAN precursor composite were stabilized, carbonized and further graphitized to produce CNT/C composites. The morphology and mechanical properties were investigated in both the precursor and carbonized states. Raman spectroscopy and electrical properties of the precursor, carbonized and graphitized composites were also analyzed.

2. Experimental

2.1. Precursor composites fabrication

CNT/PAN precursor composites were fabricated using one-step winding infiltration approach. CNT arrays were synthesized from one step chemical vapor deposition (CVD) method using FeCl_2 as catalyst [42]. The CNTs were multiwalled (MWNTs) with outer diameter of 25–60 nm, as shown in Fig. 1, and had a length of 1 mm. PAN with an average

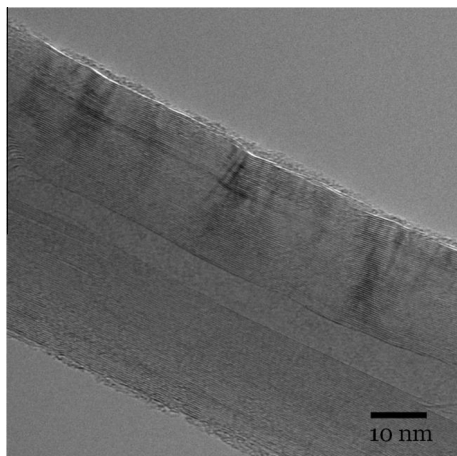


Fig. 1 – TEM image of an individual CNT.

molecular weight of 150,000 obtained from Sigma–Aldrich, was used as the matrix precursor. Dimethylformamide (DMF) (99.8%, Sigma–Aldrich) was used as solvent. CNT/PAN films with different CNT weight fractions were fabricated by using PAN/DMF solutions of different concentrations, specifically 10, 20 and 50 g/L. Unidirectional CNT sheets were drawn from spinnable CNT arrays and wound onto a rotating Polytetrafluoroethylene (PTFE) spool. During the CNT sheet winding, PAN/DMF solution droplets were applied layer by layer on the sheets to ensure sufficient infiltration. The films were then vacuum dried to remove any residual solvent and then hot-pressed at 160 °C for 2 h. The resultant samples had a thickness of 10–20 μm and were cut into strips with dimensions of 15 \times 0.5 mm.

2.2. Stabilization and pyrolysis process

The precursor films were first heat-treated in air to stabilize and oxidize the PAN matrix. A tension device was used to keep the films under tension during the heat treatment. The samples were heated to 250 °C at a heating rate of 5 °C/min and then held for 120 min, followed by heating up to 320 °C at a heating rate of 1 °C/min and then held for 25 min.

The stabilized samples were carbonized at 1300 °C in a vacuum furnace for 60 min under vacuum (below $1\text{E}-2$ mbar) after an initial ramping at 5 °C/min. A set of the samples was then heated in argon gas (99.999% and then run through an in-line $\text{O}_2/\text{H}_2\text{O}$ trap) to graphitize them. They were first heated up to 1500 °C at 25 °C/min and held for 15 min, then heated to 2000 °C at 15 °C/min and held for 15 min. Finally, the treatment temperature ramped to 2150 °C at 3 °C/min and held for 30 min. The films were sandwiched and pressed between two polished graphite plates during carbonization and graphitization.

2.3. Materials characterizations and testing

Scanning electron microscopy (SEM) analysis of the CNTs network and composite fracture surface was carried out on a JEOL 6400F microscope at an acceleration voltage of 5 kV. Raman spectra were recorded with a Renishaw Ramascope. The laser has a wavelength of 632 nm and a spot size of about 1–2 μm .

Mechanical property testing was performed using a Shimadzu EZ-S tensile testing machine at a crosshead speed of 0.5 mm/min and a gauge length of 10 mm. The sample thickness was measured with a micrometer and verified by SEM image. At least five samples were tested for each composite group. Electrical resistance was measured using the two-probe method by a 34410A 6.5 digit multimeter. Silver epoxy obtained from SRA Soldering Products was coated on the sample as an electrode.

3. Results and discussion

3.1. Mechanical properties

The mechanical properties of precursor and carbonized composites are summarized in Table 1. Fig. 2 shows the typical

stress–strain curves of composite films made using the 10 and 20 g/L PAN solutions, respectively. The strength and stiffness increased after carbonization and the tensile failure strain decreased. When using the 20 g/L concentration, the carbonized composites showed stiffness up to 143 GPa and strength up to 551 MPa, which were 200% and 58% improvement, respectively, comparing to their precursor composites. The carbonized composites obtained at both 10 and 50 g/L concentrations have lower property values, which suggests that 20 g/L may be close to the optimal concentration.

It should be noted that in the current work, CNT functionalization was purposefully avoided due to the potential damages to CNTs and the uncertainty on their effect on carbonization. Millimeter-long CNTs were used to develop effective load transfer over their length through van der Waals interactions with the matrix. In addition, high temperature has been shown to induce graphitic structure formation from PAN in the interphase region, which can improve the interaction between CNTs and the matrix. The formation of this structure is expected to enhance the mechanical properties of the composites [13,28,33,38]. The carbon matrix is more brittle than the PAN matrix making the CNT/C composites more sensitive to flaws, giving a lower failure strain in comparison to the CNT/PAN composites.

In real-world aerospace applications, a stronger and lighter material is critical in terms of saving energy and enabling advanced technologies. Typical C/C composites have a density of 1.6–2.0 g/cm⁻³ [4]. The aligned CNT/C composites presented in this study have a density of 1.1 g/cm⁻³. Consequently, their specific strength is comparable to some of the best C/C composite properties presented in the literature. The tensile strengths of previously reported CNT/C composites are far lower. The comparison is shown in Fig. 3.

3.2. Electrical properties

The electrical conductivity of C/C composites is an important property needed for some applications in aerospace composites. Although CNTs have excellent electrical conductivity, the incorporation of insulating polymer surrounding the CNTs in the composites leads to a relatively high resistance. Table 2 shows the electrical properties of the CNT/PAN precursor composites and CNT/C composite films. The carbon matrix has a much higher electrical conductivity than PAN polymer, giving rise to a much higher electrical conductivity of the CNT/C composites. It was observed that the electrical conductivity of the composites (both CNT/PAN and CNT/C) increased with decreasing concentration

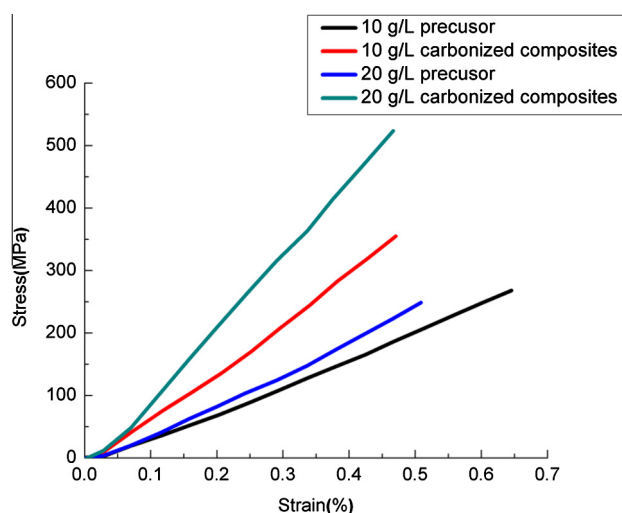


Fig. 2 – Typical stress–strain curves of precursor and carbonized composite films. (A colour version of this figure can be viewed online.)

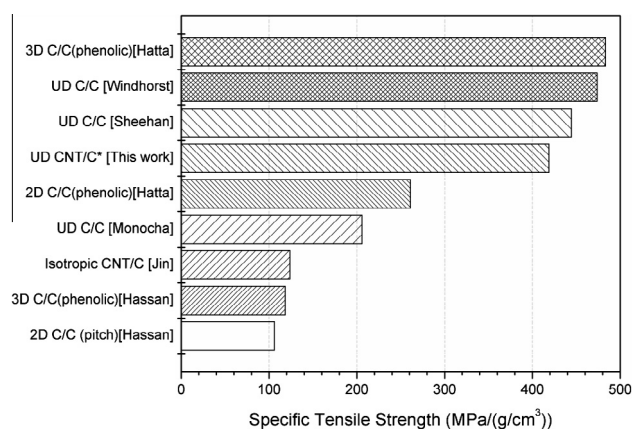


Fig. 3 – Comparison of the specific tensile strength with C/C composites and other reported CNT/C composites [2–4,13,43,44]. UD means unidirectional.

of the PAN solution. The lower solution concentrations left less polymer between CNTs after evaporation, increasing the CNT fiber volume fraction. When graphitization of the CNT/PAN composite was performed the electrical conductivity was increased by one order of magnitude, from 39 to 392 S/cm, which can be attributed to the increased graphitization degree of carbon.

Table 1 – Mechanical properties of precursor and carbonized composite films.

PAN solution concentration (g/L)	Composite sample	Young's modulus (GPa)	% Increase	Tensile strength (MPa)	Strain (%)
10	Precursor	30.0 ± 8.8	112	287.5 ± 93.4	0.85 ± 0.23
	Carbonized	63.6 ± 18.6		317.5 ± 94.1	0.56 ± 0.15
20	Precursor	31.7 ± 9.8	200	292.0 ± 51.6	1.03 ± 0.42
	Carbonized	95.2 ± 26.5		460.2 ± 96.2	0.53 ± 0.22
50	Precursor	16.2 ± 4.2	201	109.8 ± 36.6	0.80 ± 0.20
	Carbonized	48.8 ± 7.2		170.0 ± 26.5	0.61 ± 0.08

Table 2 – Electrical properties of precursor and CNT/C composite films.

PAN concentration (g/L)	Sample	Electrical resistivity (Ω cm)	Electrical conductivity (S/cm)	% Increase
10	Precursor	1.1×10^{-2}	94	289
	Carbonized	2.7×10^{-3}	368	
20	Precursor	3.1×10^{-2}	39	385
	Carbonized	8.7×10^{-3}	190	
	Graphitized	2.6×10^{-3}	392	
50	Precursor	6.5×10^{-2}	16	622
	Carbonized	8.6×10^{-3}	117	

3.3. Structural characteristics

To better understand the improvement of mechanical and electrical properties of CNT/C composites, structural characterizations were conducted. The morphology of composite films was observed using SEM. Fig. 4 shows the side view and fracture surface of the composites. High CNT volume fraction and uniform CNT distribution were observed for

the precursor composites. While the pure PAN films changed to flakes during carbonization process, the aligned CNTs provided unidirectional restriction and thus kept the stable structure of composites to sustain even higher temperature treatment. The CNT packing became denser after heat treatment due to matrix shrinkage. As the matrix underwent larger shrinkage than CNTs during pyrolysis, there was stress accumulation in the matrix, especially at the interfaces,

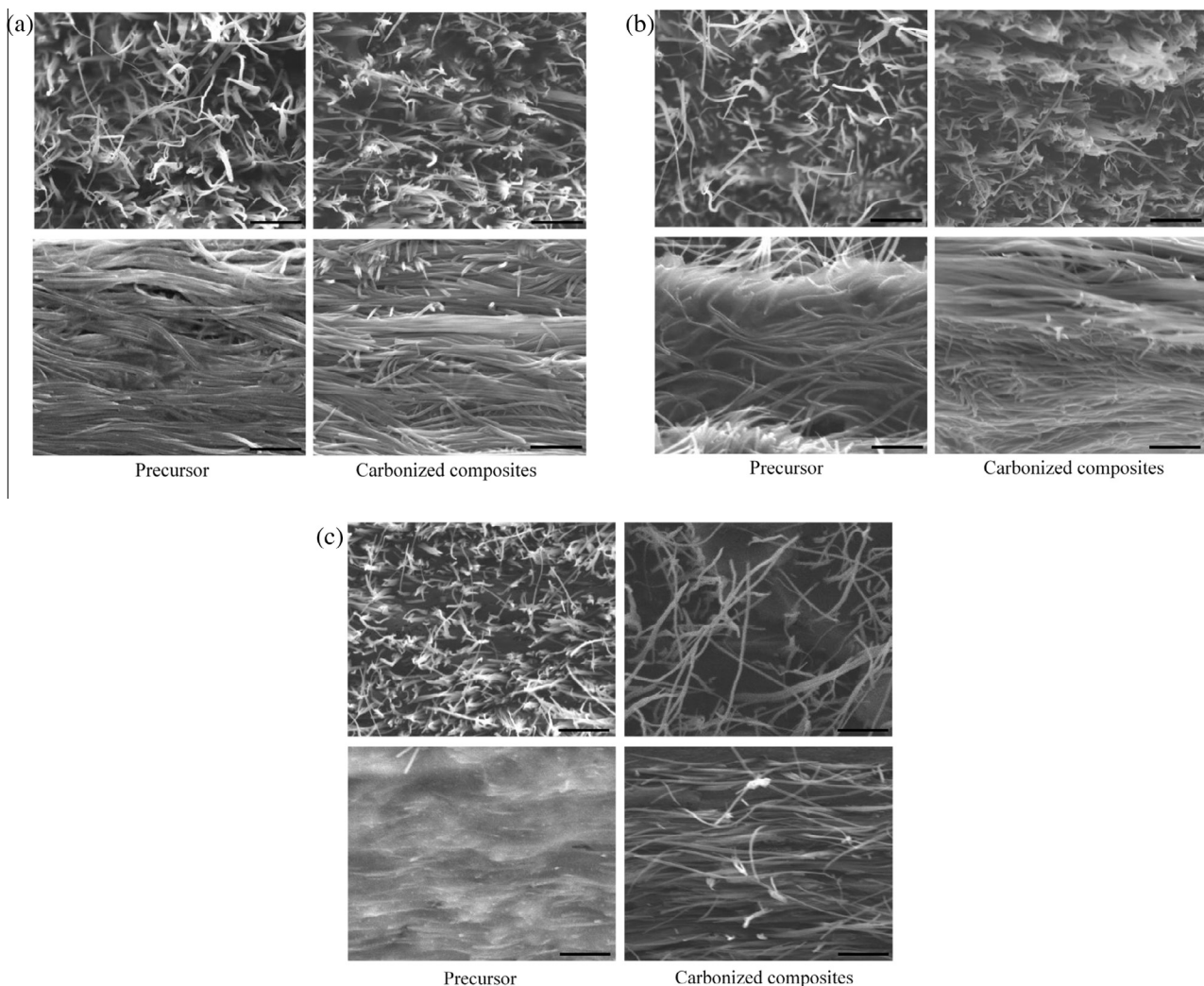


Fig. 4 – SEM images of the fracture morphologies (top) and side views (bottom) of precursor and carbonized composite films produced using 10-(a), 20-(b) and 50-g/L (c) PAN solutions. All scale bars: 1 μ m.

which was suggested to accelerate the formation of graphitic structure [21]. Better alignment of CNTs can induce higher extent of stress graphitization.

It was also observed that CNTs in carbonized composites were thicker and rougher than in the precursor composites, which may be due to individual CNTs being covered by a layer of pyrolytic or graphitic carbon. While the formation of the graphitic structure from PAN in the interphase region directly adjacent to CNT walls has been reported, the PAN matrix is mostly disordered carbon at this carbonization temperature [28,33,38]. Further investigations on the nanostructure and the formation mechanisms are needed. As compared to the precursor composites, the CNT/C composites showed shorter CNT pullout lengths. This suggests higher interfacial shear strength between CNTs and the carbon matrix, which is also supported by the higher elastic modulus of the CNT/C composites.

To further examine the heat treatment effect, Raman spectra were studied as shown in Fig. 5. The intensity ratio of graphitic G-band (at $\sim 1580\text{ cm}^{-1}$) to disorder D-band (at $\sim 1356\text{ cm}^{-1}$) is proportional to the graphite crystal size [45]. Simultaneously, the G-band peak width increases with crystal disorder. Pure PAN films and CNTs were carbonized and graphitized under the same conditions for comparison of composite films. Fig. 5a and b show the Raman spectra curves of heat-treated PAN films and CNTs, respectively. Due to functional group of PAN, it was difficult to observe the peaks for the original PAN film. As the pyrolysis temperature increased, the G-band and D-band peaks became more distinct, as shown in Fig. 5a. It should be noted that the I_G/I_D ratio was less than one, which is typical for both carbonized and graphitized PAN polymer and fibers processed at or below the temperatures used in this study [46,47]. Fig. 5b shows that the spectra of heat-treated CNTs have much sharper G-band peaks as the treatment temperature increased, indicating a more graphitic structure.

The Raman spectra of the precursor and pyrolyzed composites using 20 g/L PAN solution are shown in Fig. 5c. After heat treatment, the peak at 1320 cm^{-1} shifted to 1356 cm^{-1} , which may be due to the formation of a new carbon structure [36] or the accumulated stress at the interface [48]. Further investigation is needed to clarify this issue. When carbonized, the I_G/I_D ratio of the CNT/C composites decreased slightly and the G-band peak width increased, which may be due to the disordered carbon in the matrix (although some graphitic carbon is likely to exist adjacent to CNT walls). The significant increase in I_G/I_D ratio after graphitization suggests a higher level of graphitization, i.e. the reduction of CNT defects and the graphitization of pyrolytic carbon.

Comparing Fig. 5c and a reveals that the I_G/I_D ratios of the pyrolyzed composites were much higher than that of pure PAN films. It has been reported that the accumulated stresses in the structure due to matrix shrinkage can accelerate the atom ordering [21]. CNTs have also been reported to promote the formation of graphite-like structure [27,28,33,38]. Therefore, the higher I_G/I_D ratio may be partially attributed to the enhancement of graphitization by the introduction of aligned CNTs. Furthermore, an enhanced 1620 cm^{-1} peak was observed for the graphitized composites, which was attributed

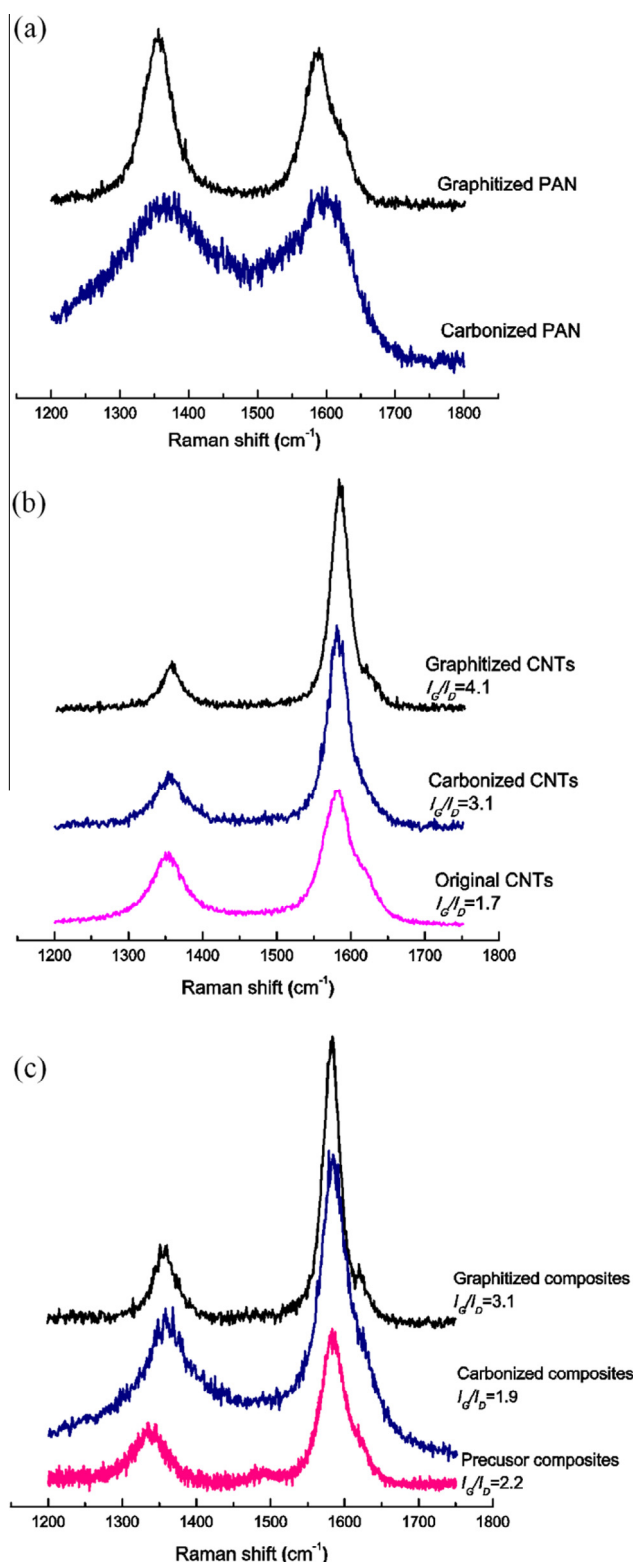


Fig. 5 – Raman spectra for (a) pyrolyzed PAN films, (b) original and heat-treated CNT arrays, and (c) precursor and pyrolyzed composite films by using 20 g/L PAN solution. (A colour version of this figure can be viewed online.)

to the structural defects [49] as pyrolytic carbon migrated and rearranged.

4. Conclusions

CNT/C composites with excellent unidirectional mechanical and electrical properties were fabricated using PAN as matrix precursor. The carbon matrix allows for more efficient load transfer in the composites than the PAN polymer matrix. The aligned and evenly distributed CNT structure obtained from one-step winding infiltration method provided a superior scaffold for the graphitization of the PAN matrix, enhancing the stress accumulation during pyrolysis and accelerating the ordering of atoms. The resultant CNT/C has increased graphitization degree than the precursor composites. With comparable specific strength to C/C composites and lower density (1.1 g/cm^{-3}), the aligned CNT/C composites produced here are promising for aerospace applications where high temperature resistance, high strength and low density are desired.

Acknowledgement

This work is supported by the Air Force Office of Scientific Research (Award# FA9550-12-1-0088).

REFERENCES

- [1] Fitzer E. The future of carbon-carbon composites. *Carbon* 1987;25(2):163–90.
- [2] Sheehan JE, Buesking KW, Sullivan BJ. Carbon-carbon composites. *Annu Rev Mater Sci* 1994;24(1):19–44.
- [3] Windhorst T, Blount G. Carbon-carbon composites: a summary of recent developments and applications. *Mater Des* 1997;18(1):11–5.
- [4] Manocha LM, Somiya S, editors. *Carbon-Carbon Composites. Handbook of Advanced Ceramics*. Oxford: Academic Press; 2013. p. 171–98. Chapter 2.10.
- [5] Iijima S. Helical microtubules of graphitic carbon. *Nature* 1991;354(6348):56–8.
- [6] Dai H, Wong EW, Lieber CM. Probing electrical transport in nanomaterials: conductivity of individual carbon nanotubes. *Science* 1996;272(5261):523–6.
- [7] Thess A, Lee R, Nikolaev P, Dai H, Petit P, Robert J, et al. Crystalline ropes of metallic carbon nanotubes. *Science-AAAS-Weekly Paper Edition* 1996;273(5274):483–7.
- [8] Baughman RH, Zakhidov AA, de Heer WA. Carbon nanotubes—the route toward applications. *Science* 2002;297(5582):787–92.
- [9] Coleman JN, Khan U, Gun'ko YK. Mechanical reinforcement of polymers using carbon nanotubes. *Adv Mater* 2006;18(6):689–706.
- [10] Yu M-F. Fundamental mechanical properties of carbon nanotubes: current understanding and the related experimental studies. *J Eng Mater-T ASME* 2004;126:271–8.
- [11] Allouche H, Monthieux M. Chemical vapor deposition of pyrolytic carbon on carbon nanotubes. Part 2. Texture and structure. *Carbon* 2005;43(6):1265–78.
- [12] Allouche H, Monthieux M, Jacobsen RL. Chemical vapor deposition of pyrolytic carbon on carbon nanotubes: Part 1. Synthesis and morphology. *Carbon* 2003;41(15):2897–912.
- [13] Jin Y, Zhang Y, Zhang Q, Zhang R, Li P, Qian W, et al. Multi-walled carbon nanotube-based carbon/carbon composites with three-dimensional network structures. *Nanoscale* 2013;5(13):6181–6.
- [14] Li X, Ci L, Kar S, Soldano C, Kilpatrick SJ, Ajayan PM. Densified aligned carbon nanotube films via vapor phase infiltration of carbon. *Carbon* 2007;45(4):847–51.
- [15] Monthieux M, Allouche H, Jacobsen RL. Chemical vapour deposition of pyrolytic carbon on carbon nanotubes: Part 3: Growth mechanisms. *Carbon* 2006;44(15):3183–94.
- [16] Gong Q-m, Li Z, Li D, Bai X-d, Liang J. Fabrication and structure: a study of aligned carbon nanotube/carbon nanocomposites. *Solid State Commun* 2004;131(6):399–404.
- [17] Song Y, Zhai G, Shi J, Guo Q, Liu L. Carbon nanotube: carbon composites with matrix derived from oxidized mesophase pitch. *J Mater Sci* 2007;42(22):9498–500.
- [18] Wu B, Wang Z, Gong QM, Song HH, Liang J. Fabrication and mechanical properties of in situ prepared mesocarbon microbead/carbon nanotube composites. *Mater Sci Eng, A* 2008;487(1):271–7.
- [19] Ye C, Gong Q-M, Lu F-P, Liang J. Preparation of carbon nanotubes/phenolic-resin-derived activated carbon spheres for the removal of middle molecular weight toxins. *Sep Purif Technol* 2008;61(1):9–14.
- [20] Hu D, Chen H, Yong Z, Chen M, Zhang X, Li Q, et al. Enhanced thermal conductivity of carbon nanotube arrays by carbonizing impregnated phenolic resins. *Mater Sci Appl* 2013;4(8).
- [21] Lanticse-Diaz LJ, Tanabe Y, Enami T, Nakamura K, Endo M, Yasuda E. The effect of nanotube alignment on stress graphitization of carbon/carbon nanotube composites. *Carbon* 2009;47(4):974–80.
- [22] Li H, Liu C, Fan S. Homogeneous carbon nanotube/carbon composites prepared by catalyzed carbonization approach at low temperature. *J Nanomater* 2010;2011:1.
- [23] Dai K, Shi L, Zhang D, Fang J. NaCl adsorption in multi-walled carbon nanotube/active carbon combination electrode. *Chem Eng Sci* 2006;61(2):428–33.
- [24] Béguin F, Szostak K, Lota G, Frackowiak E. A self-supporting electrode for supercapacitors prepared by one-step pyrolysis of carbon nanotube/polyacrylonitrile blends. *Adv Mater* 2005;17(19):2380–4.
- [25] Jagannathan S, Liu T, Kumar S. Pore size control and electrochemical capacitor behavior of chemically activated polyacrylonitrile-Carbon nanotube composite films. *Compos Sci Technol* 2010;70(4):593–8.
- [26] Liu T, Sreekumar TV, Kumar S, Hauge RH, Smalley RE. SWNT/PAN composite film-based supercapacitors. *Carbon* 2003;41(12):2440–2.
- [27] Ra EJ, Raymundo-Piñero E, Lee YH, Béguin F. High power supercapacitors using polyacrylonitrile-based carbon nanofiber paper. *Carbon* 2009;47(13):2984–92.
- [28] Prilutsky S, Zussman E, Cohen Y. The effect of embedded carbon nanotubes on the morphological evolution during the carbonization of poly (acrylonitrile) nanofibers. *Nanotechnology* 2008;19(16):165603.
- [29] Liu W, Zhang X, Xu G, Bradford PD, Wang X, Zhao H, et al. Producing superior composites by winding carbon nanotubes onto a mandrel under a poly (vinyl alcohol) spray. *Carbon* 2011;49(14):4786–91.
- [30] Wang X, Yong ZZ, Li QW, Bradford PD, Liu W, Tucker DS, et al. Ultrastrong, stiff and multifunctional carbon nanotube composites. *Mater Res Lett* 2013;1(1):19–25.
- [31] Minus M, Kumar S. The processing, properties, and structure of carbon fibers. *JOM* 2005;57(2):52–8.
- [32] Maitra T, Sharma S, Srivastava A, Cho Y-K, Madou M, Sharma A. Improved graphitization and electrical conductivity of suspended carbon nanofibers derived from carbon nanotube/polyacrylonitrile composites by directed electrospinning. *Carbon* 2011;50(5):1753–61.

- [33] Chae HG, Choi YH, Minus ML, Kumar S. Carbon nanotube reinforced small diameter polyacrylonitrile based carbon fiber. *Compos Sci Technol* 2009;69(3):406–13.
- [34] Chae HG, Sreekumar TV, Uchida T, Kumar S. A comparison of reinforcement efficiency of various types of carbon nanotubes in polyacrylonitrile fiber. *Polymer* 2005;46(24):10925–35.
- [35] Guo H, Minus ML, Jagannathan S, Kumar S. Polyacrylonitrile/carbon nanotube composite films. *ACS Appl Mater Interfaces* 2010;2(5):1331–42.
- [36] Koganemaru A, Bin Y, Agari Y, Matsuo M. Composites of polyacrylonitrile and multiwalled carbon nanotubes prepared by gelation/crystallization from solution. *Adv Funct Mater* 2004;14(9):842–50.
- [37] Koganemaru A, Bin Y, Tohora H, Okino F, Komiyama S, Zhu J, et al. Carbonization of oriented polyacrylonitrile and multiwalled carbon nanotube composite films. *Asia-Pacific J Chem Eng* 2008;3(5):521–6.
- [38] Chae HG, Minus ML, Rasheed A, Kumar S. Stabilization and carbonization of gel spun polyacrylonitrile/single wall carbon nanotube composite fibers. *Polymer* 2007;48(13):3781–9.
- [39] Liu Y, Chae HG, Kumar S. Gel-spun carbon nanotubes/polyacrylonitrile composite fibers. Part I: Effect of carbon nanotubes on stabilization. *Carbon* 2011;49(13):4466–76.
- [40] Liu Y, Chae HG, Kumar S. Gel-spun carbon nanotubes/polyacrylonitrile composite fibers. Part III: Effect of stabilization conditions on carbon fiber properties. *Carbon* 2011;49(13):4487–96.
- [41] Liu Y, Chae HG, Kumar S. Gel-spun carbon nanotubes/polyacrylonitrile composite fibers. Part II: Stabilization reaction kinetics and effect of gas environment. *Carbon* 2011;49(13):4477–86.
- [42] Inoue Y, Kakihata K, Hirono Y, Horie T, Ishida A, Mimura H. One-step grown aligned bulk carbon nanotubes by chloride mediated chemical vapor deposition. *Appl Phys Lett* 2008;92(21): 213113-3.
- [43] Aly-Hassan MS, Hatta H, Wakayama S, Watanabe M, Miyagawa K. Comparison of 2D and 3D carbon/carbon composites with respect to damage and fracture resistance. *Carbon* 2003;41(5):1069–78.
- [44] Hatta H, Goto K, Ikegaki S, Kawahara I, Aly-Hassan MS, Hamada H. Tensile strength and fiber/matrix interfacial properties of 2D- and 3D-carbon/carbon composites. *J Eur Ceram Soc* 2005;25(4):535–42.
- [45] Dresselhaus MS, Dresselhaus G, Saito R, Jorio A. Raman spectroscopy of carbon nanotubes. *Phys Rep* 2005;409(2):47–99.
- [46] Ko T-H. Raman spectrum of modified PAN-based carbon fibers during graphitization. *J Appl Polym Sci* 1996;59(4):577–80.
- [47] Lee S, Kim J, Ku B-C, Kim J, Joh H-I. Structural evolution of polyacrylonitrile fibers in stabilization and carbonization. *Adv Chem Eng Sci* 2012;2(2):275–82.
- [48] Schadler LS, Giannaris SC, Ajayan PM. Load transfer in carbon nanotube epoxy composites. *Appl Phys Lett* 1998;73(26):3842–4.
- [49] Bacsá WS, Ugarte D, Chatelain A, De Heer WA. High-resolution electron microscopy and inelastic light scattering of purified multishelled carbon nanotubes. *Phys Rev B* 1994;50(20):15473.